Journal of Alloys and Compounds 509 (2011) L319–L323

Contents lists available at ScienceDirect

Journal of Alloys and Compounds

journal homepage: www.elsevier.com/locate/jallcom

Letter

Compositionally graded bismuth ferrite thin films

Jiagang Wu[a,b,*], John Wang[b], Dingquan Xiao[a], Jianguo Zhu[a]

[a] Department of Materials Science, Sichuan University, Chengdu, 641402, PR China
[b] Department of Materials Science and Engineering, National University of Singapore, 117574, Singapore

ARTICLE INFO

Article history:
Received 5 May 2011
Received in revised form 18 May 2011
Accepted 20 May 2011
Available online 14 June 2011

Keywords:
Compositionally graded thin film
Bismuth ferrite
Multiferroic properties
Fatigue behavior

ABSTRACT

The compositionally graded $(Bi_{0.92}La_{0.08})(Fe_{1-x}Zn_x)O_3$ ($x = 0.03$, 0.07, and 0.13) thin film was layer-by-layer grown on Pt/Ti/SiO_2/Si(1 0 0) substrates without any buffer layers by radio frequency sputtering. This thin film has a pure polycrystalline perovskite structure with random orientation, a dense microstructure, and a low leakage current density. A large remanent polarization of $2P_r \sim 142.00\,\mu C/cm^2$ and a good magnetic behavior of $2M_s \sim 27.52$ emu/cm^3 are demonstrated in such a thin film. The applied electric fields and measurement frequencies strongly affect its fatigue endurance, that is, its fatigue endurance was degraded with decreasing frequencies and electric fields.

Magnetoelectric coupling in multiferroics has been recently given to considerable attention because of the intriguing physical principle underlying this phenomenon and the potential application in multiply controlled devices [1–4]. However, the known number room-temperature as well as single-phase multiferroics are still lacked [1–9]. Indeed, $BiFeO_3$ (BFO) exhibits a giant remanent polarization, a coexistence of ferroelectric and ferromagnetic parameters, a high Curie temperature of ~820 °C, and a Néel temperature of ~370 °C, promising as some practical applications in several multifunctional devices [1–9]. However, its high leakage current density and a low remanent polarization are of great challenge for developing it into a thin-film device, especially when deposited on the Pt-coated silicon substrates without any buffer layers [1–4].

The employment of site engineering [10,11], single-crystal substrates [11,12], buffer layers [11–15], and multilayer structures [16,17] has been used to effectively reduce the leakage current, and some promising results were also demonstrated. However, some shortcomings still affect its practical applications although its leakage current can be suppressed by these methods mentioned above. For example, the site engineering usually results in the degradation of the polarization of BFO although its leakage current can be greatly suppressed [5]; the use of single-crystal substrates and buffer layers improves the electrical properties of BFO, but expensive costs and a high processing temperature hinder the practical application in the silicon integration technique [11,12]. The multilayer structure approach is among the most leading approaches-going topics, whereby the coupling and interactions among different functional layers in multilayers can strongly influence the growth and physical properties of these films [16,17]. Indeed, an appropriate combination of nanolayers differing in composition or structure can lead to a dramatic enhancement in multiferroic behavior. Especially multilayers with a compositional fluctuation across the thickness exhibits striking properties that were not observed in conventional ferroelectric films [18,19].

In the present work, the compositionally graded $(Bi_{0.92}La_{0.08})(Fe_{1-x}Zn_x)O_3$ ($x = 0.03$, 0.07, and 0.13) (BLFZO) thin films were layer-by-layer fabricated on Pt/Ti/SiO_2/Si(1 0 0) substrates by radio frequency (rf) magnetron sputtering, where it is difficult to prepare the bismuth ferrite thin films with good electrical properties when grown on the Pt-coated silicon substrate without any buffer layers by rf sputtering [17]. A pure phase, a dense microstructure, and a low leakage current density are well established in such a compositionally graded thin film. A larger remanent polarization, a better magnetic behavior, and an improved fatigue behavior are demonstrated in such a compositionally graded thin film.

Firstly, three kinds of $(Bi_{1.00}La_{0.10})(Fe_{1-x}Zn_x)O_3$ ($x = 0.05$, 0.10, and 0.15) targets were prepared by the conventional solid-state reaction process, and the preparation parameter for ceramic targets and thin films has been described elsewhere [20]. The stacking sequence of the compositionally graded thin film is as follows: $(Bi_{0.92}La_{0.08})(Fe_{0.87}Zn_{0.13})O_3/(Bi_{0.92}La_{0.08})(Fe_{0.93}Zn_{0.07})O_3/(Bi_{0.92}La_{0.08})(Fe_{0.97}Zn_{0.03})O_3$/Pt/Ti/$SiO_2$/Si(1 0 0), where the composition for each layer is analyzed by EDX. The rf magnetic

* Corresponding author at: Department of Materials Science, Sichuan University, Chengdu, 641402, PR China.
E-mail addresses: wujiagang0208@163.com, msewujg@scu.edu.cn (J. Wu).

0925-8388/$ – see front matter © 2011 Elsevier B.V. All rights reserved.
doi:10.1016/j.jallcom.2011.05.076

sputtering was used to *in situ* prepare the compositionally graded thin film on Pt/Ti/SiO_2/Si(1 0 0) substrates by two-inch targets of $(Bi_{1.00}La_{0.10})(Fe_{1-x}Zn_x)O_3$. The $(Bi_{0.92}La_{0.08})(Fe_{1-x}Zn_x)O_3$ (x = 0.03, 0.07, and 0.13) layers were deposited on Pt/TiO_2/SiO_2/Si substrates at 580 °C, 560 °C, and 530 °C, respectively. The $(Bi_{0.92}La_{0.08})(Fe_{1-x}Zn_x)O_3$ (x = 0.03, 0.07, and 0.13) layers are ~150 nm, ~100 nm, and ~50 nm in thickness, respectively. Circular Au electrodes of 0.2 mm in diameter were sputtered on film surface using a shadow mask. The phases were analyzed by using X-ray diffraction (Bruker D8 Advanced XRD, Bruker AXS Inc., Madison, WI, CuKa). Field emission scanning electron microscopy (Philips, XL30) was employed to study their surface morphologies. An impedance analyzer (Solartron Grain Phase Analyzer) was employed to characterize their dielectric behavior. Their leakage current was measured by using a Keithley meter (Keithley 6430, Cleveland, OH). Their fatigue and ferroelectric properties were studied by using the Radiant precise workstation (Radiant Technologies, Medina, NY). Their magnetic properties were characterized by using a superconducting quantum interference device (SQUID, MPMS, XL-5AC, San Diego, CA).

Fig. 1(a) shows XRD patterns of single layers and compositionally graded thin films. All films are of a pure phase. The $(Bi_{0.92}La_{0.08})(Fe_{0.97}Zn_{0.03})O_3$ thin film is of a polycrystalline structure with random orientation, while $(Bi_{0.92}La_{0.08})(Fe_{1-x}Zn_x)O_3$ (x = 0.07 and 0.13) thin films are of a polycrystalline structure with a (1 1 0) orientation. However, the compositionally graded thin film has a polycrystalline structure with random orientation, owing to the induced growth of the bottom $(Bi_{0.92}La_{0.08})(Fe_{0.97}Zn_{0.03})O_3$ layer. Fig. 1(b) shows enlarged XRD patterns for all films. The $(Bi_{0.92}La_{0.08})(Fe_{1-x}Zn_x)O_3$ (x = 0.03, 0.07, and 0.13) phases were well retained in this compositionally graded thin film. The La^{3+} (1.18 Å) and Zn^{2+} (0.74 Å) substitutions respective for Bi^{3+} (1.03 Å) and Fe^{2+} (0.55 Å) sites result in the shift of diffraction peaks due to a larger ion radius, confirming that La^{3+} and Zn^{2+} are dissolved in BFO lattice. In addition, the positions of the 2θ diffraction angles in the compositionally graded thin film were found to be in between those of these films. Fig. 1(c) shows the surface morphology of the compositionally graded thin film. The film appears to be dense, crack-free, and well adhered on the Pt-coated silicon substrate, where the grains with long shape are parallel to the substrate and these large grains were surrounded by small grains. Fig. 1(d) shows the SEM micrograph of the cross section for the compositionally graded thin film. The film is ~300 nm in thickness, and the interface between the film and Pt electrode is clear. The dense microstructure is also a contribution parameter for the dramatic reduction in the leakage current of the compositionally graded thin film.

Fig. 2(a) shows J–E curves for single layers and compositionally graded thin film. The leakage current almost kept unchanged for all films in low electric field regions (E < 50 kV/cm), while all films exhibit different leakage behavior in high electric field regions (E > 50 kV/cm). The compositionally graded thin film exhibits a lowest leakage current density in high electric field regions, and possesses a low leakage current density of 1.39×10^{-4} A/cm^2 at $E \sim 160$ kV/cm, due to dense microstructure. Fig. 2(b) plots magnetic properties of single-layer and compositionally graded thin film. The magnetic properties of single layers were degraded with increasing Zn content, owing to an increase in the nonmagnetic composition of Zn. In contrast, the compositionally graded thin film has better magnetic properties than those of $(Bi_{0.92}La_{0.08})(Fe_{1-x}Zn_x)O_3$ single layers. The Zn^{2+} substitution for the Fe site in BFO generates the more concentration of oxygen vacancies and suppresses the formation of Fe^{2+} [9,20], and then the impure Fe^{2+} in each layer cannot contribute to the increase in the magnetic properties of the compositionally graded thin film [21]. Therefore, the enhanced magnetic properties should be attributed to the interface coupling among three consisting layers in the compositionally graded thin film in this work. Fig. 2(c) plots P–E loops of compositionally graded thin film, measured at room temperature and 3.3 kHz. The compositionally graded thin film exhibits a saturated ferroelectric behavior, where a large remnant polarization of $2P_r \sim 142.00\ \mu C/cm^2$ was obtained together with $2E_c \sim 661.67$ kV/cm. The inset in Fig. 2(c) shows the plots of $2P_r$ and $2E_c$ values as a function of applied electric fields for the compositionally graded thin film. The $2P_r$ values were firstly obtained at the electric field of higher than ~80 kV/cm, the $2P_r$ values increase quickly with increasing electric fields from ~80 kV/cm to ~600 kV/cm, and then slightly change with further increasing electric fields, indicating the saturation of P–E curves. A similar polarization value was also demonstrated by PUND as compared to that measured by P–E hysteresis loop, as shown in the insets in Fig. 2(c), confirming that the leakage current does not affect the ferroelectric behavior of the compositionally graded thin film. The compositionally graded thin film demonstrated the large $2P_r$ value of ~142.00 μC/cm^2, which is higher than those that have been reported for BFO single layers and multilayers [11,15–17]. Some factors affected the ferroelectric behavior of BFO, such as orientation [12], crystal structure [22], buffer layer [11–15], multilayer structure [16,17], and ion substitutions [23,24]. In this work, the crystal structure, buffer layer, and orientation cannot largely contribute to the improvement in the polarization of the compositionally graded thin film, because no any buffer layers were applied to the film and the polycrystalline structure with random orientation was only induced. Usually, bad P–E loops were obtained for the BFO directly deposited on Pt-coated silicon substrates [17]. Therefore, the ion substitution should largely contribute to the improvement in ferroelectric properties of the compositionally graded thin film by dramatically reducing the leakage current, where the low leakage current benefits to obtain intrinsic polarization value. The multilayer structure helps improve electrical properties by the interface coupling among three consisting layers and reduced leakage current [16,17].

Fig. 3(a) shows the frequency dependence of fatigue behavior in the compositionally graded thin film at $E \sim 333$ kV/cm. Its fatigue behavior strongly depends on measurement frequencies. At f = 1 MHz, the film exhibits fatigue-free at a switching cycle of ~10^{10}, and the fatigue endurance was slightly degraded with a decrease at f = 300 kHz. However, with further decreasing frequencies (f = 100 kHz), the polarization value increases dramatically with the number of switching cycles. The "wake up" peak is formed and is shifted to a lower switching cycle with a decrease in f from 100 kHz to 10 kHz. Such an unusual fatigue behavior in multilayers is related to the higher leakage current and the space charge [25,26]. In order to illuminate this "wake up" phenomenon, the dielectric and resistivity behavior before and after fatigue at different switching frequencies were measured for the compositionally graded thin film, as shown in Fig. 3(c)–(e). The obviously different dielectric behavior is demonstrated with varied frequencies. The dielectric behavior and resistivity are slightly changed after a high-frequency (1 MHz) fatigue. However, a big difference in dielectric and resistivity behavior was observed in a low frequency region after a low-frequency (100 kHz and 50 kHz) fatigue, and the large dielectric relaxation in a low frequency region indicates the involvement of more space charge after a low frequency fatigue, confirming that space charge is responsible for the "wake up" phenomenon [17,25,27,28]. Moreover, the resistivity in a low frequency region becomes lower with decreasing frequencies, indicating the increase of the defect concentration after fatigue. As shown in Fig. 3(b), the P–E loops before and after a low frequency polarization switching indicate that there is an increase in P_r value due to an increase in the conductivity, while the P_r value is almost kept unchanged due to a slight change in the conductivity after a high frequency polarization switching.

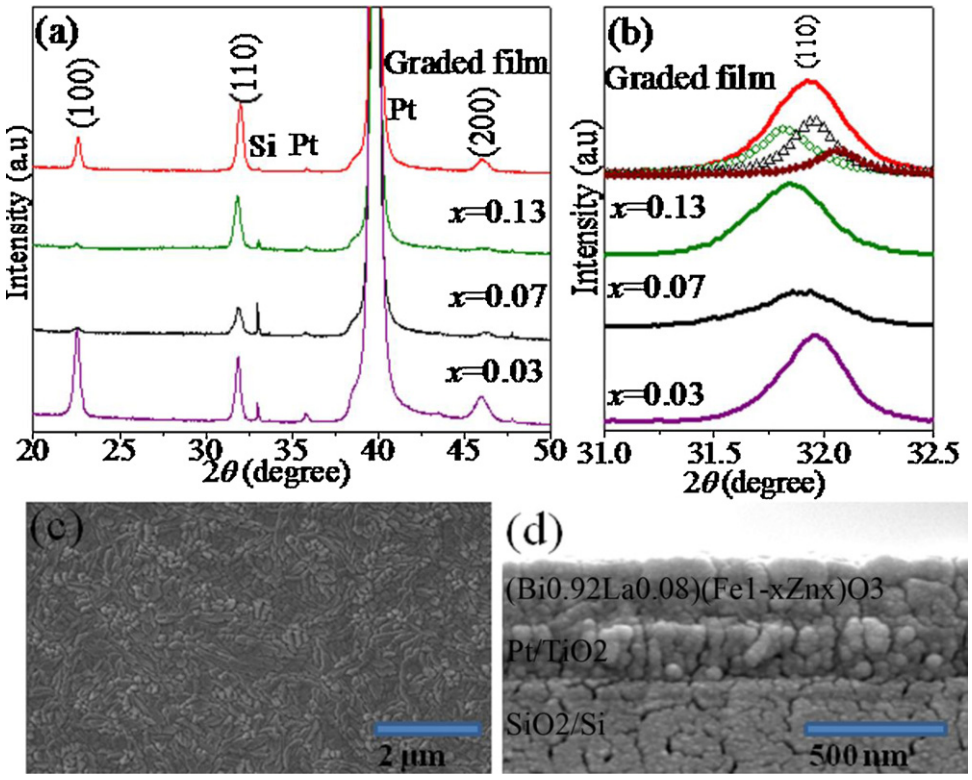

Fig. 1. (a) XRD patterns and (b) enlarged XRD patterns in the 2θ range of 31.0–32.5° for single layers and compositionally graded thin films. (c) Surface morphology and (d) cross section of the compositionally graded thin film.

Fig. 4(a) shows the field dependence of fatigue behavior in compositionally graded thin film at $f \sim 100$ kHz. At $E \leq 300$ kV/cm, the film exhibits a poor fatigue behavior, as confirmed by P–E loops before and after fatigue [Fig. 4(b)]. In contrast, its fatigue endurance was greatly improved with increasing applied electric fields of $E > 300$ kV/cm, and the unusual "wake up" phenomenon was observed at $E \geq 380$ kV/cm. A higher applied electric field can facilitate the depinning and easily reverse the domains, generating a better fatigue endurance. The competition between the domain wall pinning and depinning dominates fatigue mechanism. Similar phenomenon was also found in La-modified BFO films [29]. Moreover, the fatigue behavior is also dominated by space charge layers in each case, while such space charge accumulates at the layer interfaces of multilayers, rather than at the electrode–dielectric interface [30]. The dielectric and resistivity behavior before and after fatigue at different applied electric fields were also characterized for the compositionally graded thin film for identifying the involvement of the space charge, as plotted in Fig. 4(c)–(e), the

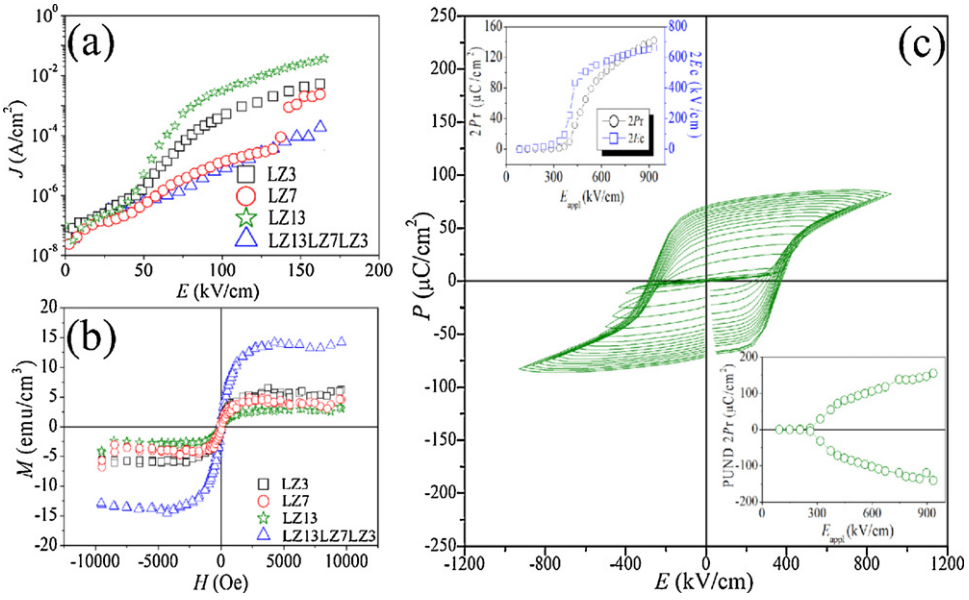

Fig. 2. (a) J–E curves and (b) magnetic properties for single layers and compositionally graded thin films. (c) P–E curves, where the insets are $2P_r$ and $2E_c$ values as a function of applied electric fields, and PUND curve of the compositionally graded thin film.

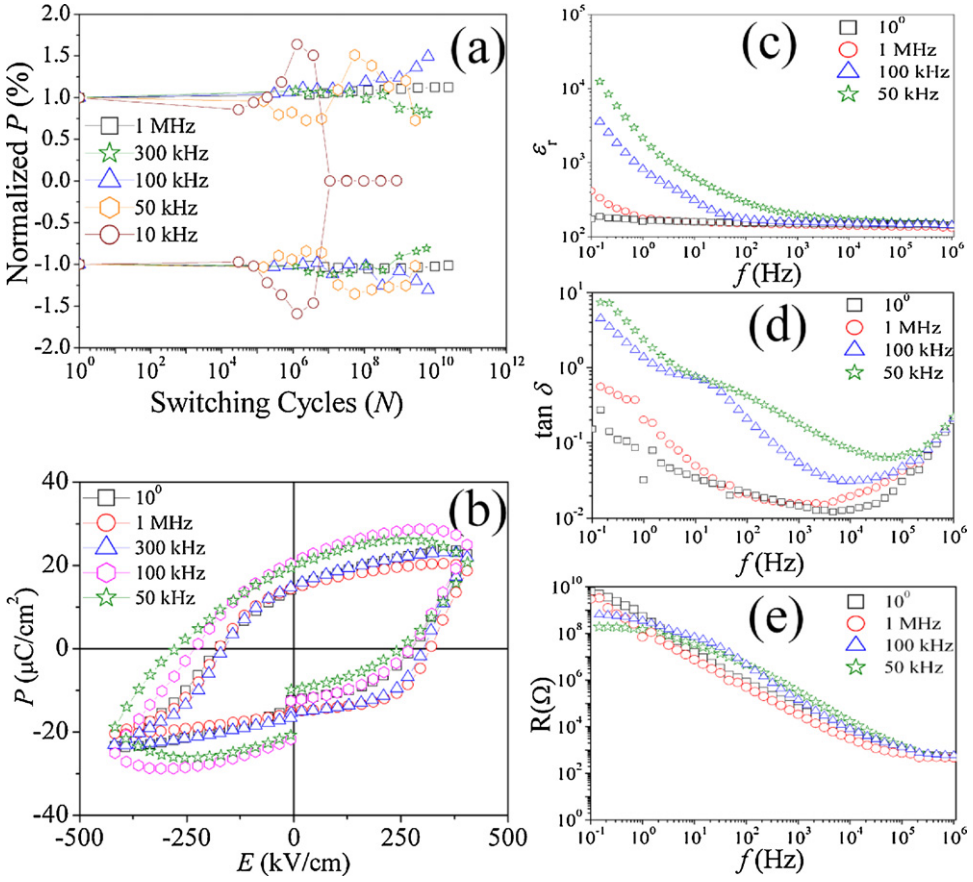

Fig. 3. (a) Frequencies-dependent fatigue behavior, (b) *P*–*E* loops before and after fatigue endurance, (c) ε_r vs. *f*, (d) tan δ vs. *f*, and (e) *R* vs. *f* of the compositionally graded thin film.

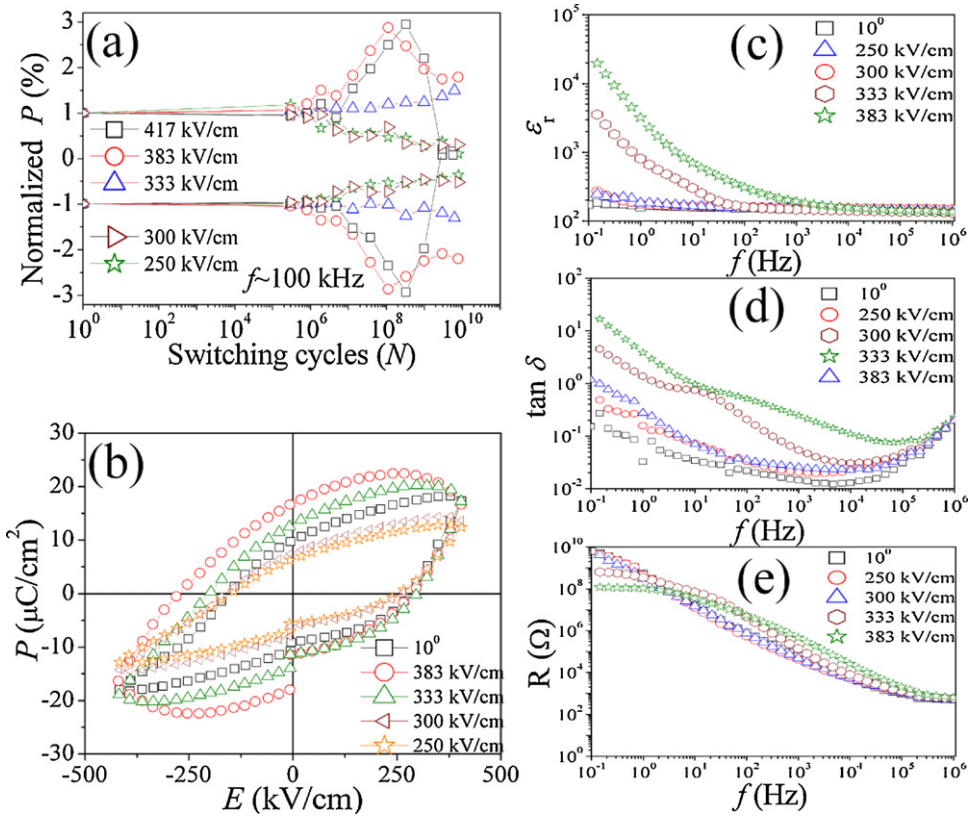

Fig. 4. (a) Electric fields-dependent fatigue behavior, (b) *P*–*E* loops before and after fatigue endurance, (c) ε_r vs. *f*, (d) tan δ vs. *f*, and (e) *R* vs. *f* of the compositionally graded thin film.

low frequency dielectric relaxation indicates the involvement of more pace charge polarization after a high electric field polarization switching, indicating that the space charge is also responsible for the "wake up" phenomenon and the improvement of fatigue endurance in a high-field polarization switching. In a low driving field of $E < 300$ kV/cm, the dielectric behavior and resistivity almost kept unchanged, indicating the involvement of few space charge accumulating at the layer interfaces. As shown in Fig. 4(c)–(e), the "wake up" phenomenon after a high-field polarization switching should be also due to the involvement of more space charge and higher conductivity. Therefore, the higher driving fields, the better fatigue endurance.

In summary, the compositionally graded $(Bi_{0.92}La_{0.08})(Fe_{1-x}Zn_x)O_3$ ($x = 0.03$, 0.07, and 0.13) thin films were grown on $Pt/Ti/SiO_2/Si(1\,0\,0)$ substrates by radio frequency sputtering. The compositionally graded thin film exhibits a pure polycrystalline perovskite structure with random orientations, low leakage current density and dense microstructure. A larger remanent polarization was induced in the compositionally graded thin film by the low leakage current and the interface coupling among three consisting layers, together with a good magnetic behavior. The electric fields and frequencies dependence of fatigue endurance indicates the fatigue endurance of the compositionally graded thin film endurance degraded with a decrease in frequencies and electric fields.

Acknowledgements

Dr. Jiagang Wu gratefully acknowledges the supports of the introduction of talent start funds of Sichuan University (2082204144033), the Sichuan University, and the National University of Singapore. Thank reviewers and editor for their good comments and advice, which benefit to the improvement of our paper.

References

[1] R. Ramesh, N.A. Spaldin, Nature 6 (2007) 21.
[2] W. Eerenstein, N.D. Mathur, J.F. Scott, Nature 442 (2006) 759.
[3] L.W. Martin, Y.H. Chu, R. Ramesh, Mater. Sci. Eng. R 68 (2010) 89.
[4] G. Catalan, J.F. Scott, Adv. Mater. 21 (2009) 2463.
[5] K.F. Wang, J.M. Liu, Z.F. Ren, Adv. Phys. 58 (2009) 321.
[6] C.W. Nan, M.I. Bichurin, S.X. Dong, D. Viehland, G. Srinivasan, J. Appl. Phys. 103 (2008) 031101.
[7] J.F. Li, J.L. Wang, M. Wuttig, R. Ramesh, N. Wang, B. Ruette, A.P. Pyatakov, A.K. Zvezdin, D. Viehland, Appl. Phys. Lett. 84 (2004) 5261.
[8] H. Yang, M. Jain, N.A. Suvorova, H. Zhou, H.M. Luo, D.M. Feldmann, P.C. Dowden, R.F. DePaula, S.R. Foltyn, Q.X. Jia, Appl. Phys. Lett. 91 (2007) 072911.
[9] X.D. Qi, J. Dho, R. Tomov, M.G. Blamire, J.L. MacManus-Driscoll, Appl. Phys. Lett. 86 (2005) 062903.
[10] S.K. Singh, K. Maruyama, H. Ishiwara, J. Phys. D 40 (2007) 2705.
[11] J. Wang, J.B. Neaton, H. Zheng, V. Nagarajan, S.B. Ogale, B. Liu, D. Viehland, V. Vaithyanathan, D.G. Schlom, U.V. Waghmare, N.A. Spaldin, K.M. Rabe, M. Wuttig, R. Ramesh, Science 299 (2003) 1719.
[12] J.G. Wu, J. Wang, J. Appl. Phys. 106 (2009) 104111.
[13] H. Béa, M. Bibes, S. Fusil, K. Bouzehouane, E. Jacquet, K. Rode, P. Bencok, A. Barthélémy, Phys. Rev. B 74 (2006) 020101(R).
[14] J.G. Wu, J. Wang, Acta. Mater. 58 (2010) 1688.
[15] Y.H. Lee, J.M. Wu, Y.L. Chueh, J. Chou, Appl. Phys. Lett. 87 (2005) 172901.
[16] H.Y. Zhao, H. Kimura, Z.X. Cheng, X.L. Wang, T. Nishida, Appl. Phys. Lett. 95 (2009) 232904.
[17] J.G. Wu, G.Q. Kang, H.J. Liu, J. Wang, Appl. Phys. Lett. 94 (2009) 172906.
[18] R. Ranjith, A. Laha, S.B. Krupanidhi, Appl. Phys. Lett. 86 (2005) 092902.
[19] V.M. Petrov, G. Srinivasan, Phys. Rev. B 78 (2008) 184421.
[20] J.G. Wu, J. Wang, Electrochem. Solid-State Lett. 13 (2010) G105.
[21] W. Eerenstein, F.D. Morrison, J. Dho, M.G. Blamire, J.F. Scott, N.D. Mathur, Science 307 (2005) 1203.
[22] K.Y. Yun, D. Ricinschi, T. Kanashima, M. Noda, M. Okuyama, Jpn. J. Appl. Phys. 43 (2004) L647.
[23] S.K. Singh, K. Maruyama, H. Ishiwara, Appl. Phys. Lett. 91 (2007) 112913.
[24] J.G. Wu, J. Wang, J. Appl. Phys. 106 (2009) 054115.
[25] C.H. Sim, Z.H. Zhou, X.S. Gao, H.P. Soon, J. Wang, J. Appl. Phys. 103 (2008) 034102.
[26] D. Damjanovic, Rep. Prog. Phys. 61 (1998) 1267.
[27] J.F. Scott, M. Dawber, Appl. Phys. Lett. 76 (2000) 3801.
[28] M. Dawber, J.F. Scott, Appl. Phys. Lett. 76 (2000) 1060.
[29] Y. Wang, R.Y. Zheng, C.H. Sim, J. Wang, J. Appl. Phys. 105 (2009) 016106.
[30] A.Q. Jiang, Y.Y. Lin, T.A. Tang, J. Appl. Phys. 102 (2007) 074109.